UDK 620.3:544.537
Original scientific article/Izvirni znanstveni članek

ISSN 1580-2949
Mater. Tehnol.

STRUCTURAL AND VIBRATIONAL PROPERTIES OF PLAL-SYNTHESIZED GaSe NANOPARTICLES ON DIFFERENT SUBSTRATES

STRUKTURNE IN VIBRACIJSKE LASTNOSTI NANODELCEV GaSe, SINTETIZIRANIH Z METODO PLAL, NA RAZLIČNIH PODLAGAH

Marjetka Conradi[1], Vagif Salmanov[2], Rovshan Mamedov[2], Ali Guseinov[2], Fidan Ahmedova[2], Lamiya Balayeva[2], Mahammad Baghir Baghirov[3], Aydan Khaligzade[4,5], Zeynab Addayeva[3]

[1]Institute of Metals and Technology, Lepi pot 11, 1000 Ljubljana, Slovenia
[2]Department of Semiconductor physics, Baku State University, 23 Academic Zahid Khalilov Street, Baku AZ1148, Azerbaijan
[3]Nano Research Laboratory, Baku State University, 23 Academic Zahid Khalilov Street, Baku AZ1148, Azerbaijan
[4]Institute of Physics, Ministry of Science and Education, Baku AZ1143, Azerbaijan
[5]Azerbaijan University of Architecture and Construction Ayna Sultanova street 5, Az1073, Baku, Azerbaijan

Prejem rokopisa – received: 2026-06-08; sprejem za objavo – accepted for publication: 2026-075-03

doi:10.17222/mit.2026.1766

GaSe nanoparticles were synthesized by pulsed-laser ablation in liquid (PLAL) using Bridgman-grown GaSe single crystals as targets. The laser ablation was performed in distilled water using a Nd:YAG laser operating at a wavelength of 1064 nm, pulse energy of 135 mJ, pulse duration of 10 ns, and repetition rate of 10 Hz. The structural, morphological, compositional, and vibrational properties of the synthesized nanoparticles deposited on glass and silicon substrates were investigated by XRD, SEM, EDS, and Raman spectroscopy. XRD analyses confirmed the preservation of the hexagonal ε-GaSe phase with crystallite sizes of approximately 10–30 nm. SEM observations revealed quasi-spherical nanoparticles with dimensions in the nanometer range, while EDS verified the presence of Ga and Se without detectable impurity phases. Raman measurements demonstrated the retention of the characteristic GaSe phonon modes and revealed substrate-dependent variations in the vibrational response of the nanoparticle layers. These results demonstrate that PLAL is an effective method for producing crystalline GaSe nanoparticles while preserving the fundamental structural characteristics of the parent material. The observed substrate-dependent behavior highlights the potential of GaSe nanostructures for future optoelectronic and nanophotonic applications.

Keywords: GaSe nanoparticles; Pulsed laser ablation in liquid (PLAL); Layered semiconductor; Substrate-dependent vibrational properties;

V tem delu so bili nanodelci GaSe sintetizirani z metodo pulzne laserske ablacije v tekočini (PLAL), pri čemer so bili kot tarče uporabljeni monokristali GaSe, vzgojeni po Bridgmanovi metodi. Laserska ablacija je bila izvedena v destilirani vodi z laserjem Nd:YAG, ki je deloval pri valovni dolžini 1064 nm, energiji pulza 135 mJ, trajanju pulza 10 ns in frekvenci ponavljanja 10 Hz. Strukturne, morfološke, sestavne in vibracijske lastnosti sintetiziranih nanodelcev, nanesenih na steklene in silicijeve substrate, so bile preučene z rentgensko difrakcijo (XRD), vrstično elektronsko mikroskopijo (SEM), energijsko disperzijsko rentgensko spektroskopijo (EDS) in Ramansko spektroskopijo. Analiza XRD je potrdila ohranitev heksagonalne faze ε-GaSe z velikostjo kristalitov približno med 10 in 30 nm. Opazovanja s SEM so pokazala kvazisferične nanodelce nanometrskih dimenzij, medtem ko je analiza EDS potrdila prisotnost galija (Ga) in selena (Se) brez zaznavnih nečistotnih faz. Ramanske meritve so pokazale ohranitev značilnih fononskih načinov GaSe ter razkrile od substrata odvisne spremembe v vibracijskem odzivu plasti nanodelcev. Rezultati kažejo, da je metoda PLAL učinkovita za pripravo kristaliničnih nanodelcev GaSe ob hkratnem ohranjanju temeljnih strukturnih značilnosti izvornega materiala. Opaženo od substrata odvisno obnašanje poudarja potencial nanostruktur GaSe za prihodnje optoelektronske in nanofotonske aplikacije.

Ključne besede: nanodelci GaSe pulzna laserska ablacija v tekočini (PLAL); slojeviti polprevodnik; od substrata odvisne vibr;acijske lastnosti

1 INTRODUCTION

Gallium selenide (GaSe) is a layered III–VI semiconductor characterized by a unique crystal architecture composed of covalently bonded atomic planes arranged in a Se–Ga–Ga–Se sequence within each tetralayer unit and weakly coupled to adjacent layers through van der Waals (vdW) interactions.[1–3] This highly anisotropic structure, defined by in-plane lattice parameters a = b ≈ 0.374 nm and a fundamental layer thickness of approximately 0.9 nm, enables mechanical exfoliation down to few-layer and monolayer regimes while preserving a high crystalline quality.[4] Variations in tetralayer stacking order give rise to multiple polytypes, including β-, ε-, and γ-GaSe, each exhibiting distinct symmetry-dependent optical and electronic characteristics.[5] Owing to its strong intrinsic nonlinear optical response, broad optical transparency from the visible to the near-infrared spectral range, and high photosensitivity, GaSe has emerged as a promising material platform for nonlinear photonics,

*Corresponding author's e-mail:
marjetka.conradi@imt.si

© 2026 The Author(s). Except when otherwise noted, articles in this journal are published under the terms and conditions of the Creative Commons Attribution 4.0 International License (CC BY 4.0).

ultrafast optoelectronics, and terahertz radiation technologies.[6,7] Furthermore, high-quality GaSe single crystals can be readily synthesized via the Bridgman technique, yielding atomically flat, mechanically stable layered surfaces that facilitate device integration.[8]

Reducing layered semiconductors into nanoscale building blocks has attracted considerable attention due to size-dependent quantum confinement effects, enhanced surface-to-volume ratios, and tunable optoelectronic properties.[9,10] GaSe nanoparticles, in particular, are expected to exhibit a modified band structure, a strengthened light–matter interaction, and improved carrier dynamics, offering new opportunities for high-performance photodetectors, nonlinear optical components, and nanophotonic devices.[11,12] However, conventional chemical synthesis routes, such as sol–gel, hydrothermal, and chemical precipitation methods, often rely on complex precursor chemistry, surfactants, and reducing agents that may introduce impurities, surface contamination, and structural disorder, which are especially detrimental for layered semiconductors where interfacial integrity plays a critical role in determining the electronic and optical behavior.[13,14] To overcome these limitations, laser ablation in liquids (LALs) has emerged as a powerful, top-down physical approach for producing high-purity, ligand-free semiconductor nanoparticles.[15,16] In this method, intense pulsed-laser irradiation of a solid target immersed in a liquid medium induces localized plasma formation, followed by rapid quenching and condensation of the ablated species into nanoscale particles. The ultrafast cooling rates and confined growth environment enable the formation of crystalline nanoparticles while minimizing oxidation and chemical contamination.[17] Unlike chemical synthesis techniques, LAL does not require precursor compounds, stabilizing agents, or post-synthesis purification, making it particularly suitable for sensitive layered materials such as GaSe. Moreover, the intrinsic anisotropic bonding nature of GaSe–strong covalent intralayer interactions combined with weak vdW interlayer coupling–facilitates laser-induced ablation followed by plasma-mediated condensation into nanoscale domains, promoting the formation of structurally coherent nanoparticles. By tuning laser parameters such as the pulse energy, wavelength, and ablation medium, the particle size, morphology, and crystallinity can be precisely controlled, enabling systematic tailoring of GaSe nanostructures for targeted optoelectronic functionalities.[18]

We report the synthesis of GaSe nanoparticles via the laser ablation of bulk GaSe single crystals in liquid media. Following laser-ablation synthesis, the as-prepared GaSe nanoparticles were deposited onto conventional glass and silicon substrates and dried under ambient atmospheric conditions to form uniform nanoparticle layers suitable for comprehensive characterization. This approach enables the direct investigation of substrate-dependent structural and optical behavior while preserving the intrinsic properties of the laser-generated nanomaterials. Systematic comparisons were performed between GaSe nanoparticles on different substrates as well as with bulk GaSe single crystals to elucidate size-induced modifications, interfacial effects, and the confinement-driven property evolution. Such a comparative analysis provides critical insights into the transformation of GaSe from a layered bulk semiconductor into nanoscale building blocks and clarifies the role of substrate interactions in governing the functional performance of GaSe-based nanostructures.

2 EXPERIMENTAL PART

2.1 Synthesis of GaSe nanoparticles by LAL

GaSe nanoparticles were synthesized via pulsed-laser ablation in liquid (PLAL). High-quality GaSe single crystals were grown in our laboratory using the horizontal Bridgman method and subsequently employed as targets for laser ablation. Owing to the layered nature of GaSe, thin plate-like targets were obtained by mechanical cleavage from bulk crystals, yielding optically smooth, mirror-like surfaces with typical thicknesses of approximately 100 μm. Such surfaces ensured stable and reproducible laser–matter interaction during the ablation process.

Laser irradiation was performed using a pulsed Nd:YAG laser system (LQ529B) equipped with second- and third-harmonic generation modules, enabling operation at wavelengths of (1064, 532 and 355) nm. In the present study, nanoparticle synthesis was carried out at the fundamental wavelength (λ = 1064 nm). The incident laser fluence was controlled using calibrated neutral-density filters to regulate the energy delivered to the target surface. For ablation, the cleaved GaSe target was placed in a quartz cuvette filled with distilled water and irradiated using a pulse duration of 10 ns, pulse energy of 135 mJ, repetition rate of 10 Hz, and an exposure time of approximately 10 min. The laser beam was focused onto the target surface to produce a spot diameter of approximately 2 mm. Based on the pulse energy, the corresponding laser fluence was estimated to be approximately 4.3 J cm^{-2}.

The formation of GaSe nanoparticles during PLAL proceeds through a sequence of laser-induced ablation, plasma-generation, nucleation, and particle-growth processes. Upon irradiation, the laser energy is absorbed by the GaSe target, resulting in rapid localized heating of the irradiated region. When the surface temperature exceeds the melting and vaporization thresholds, material is removed from the target through laser ablation, leading to the ejection of Ga- and Se-containing species into the surrounding liquid medium. Under these conditions, a transient plasma plume consisting of atoms, ions, clusters, and electrons is generated above the target surface. The liquid environment strongly confines the plasma, promoting rapid expansion followed by ultrafast cooling.

This rapid quenching creates supersaturation of the ablated species and initiates nucleation processes within the liquid. Subsequent condensation and coalescence of the plasma-derived species lead to the formation of nanoscale GaSe particles dispersed throughout the liquid medium. The liquid environment simultaneously limits excessive particle growth and aggregation, enabling the formation of nanoparticles with dimensions in the nanometer range.

A schematic illustration of the experimental setup and the proposed nanoparticle formation mechanism is presented in Figure 1a, while photographs of the resulting GaSe colloidal suspension and the parent bulk crystal are shown in Figure 1b and Figure 1c, respectively. After nanoparticle generation, the obtained colloidal suspension was transferred into a separate container containing pre-cleaned glass and silicon substrates. The suspension was allowed to spread naturally over the substrate surfaces and was subsequently dried under ambient atmospheric conditions at room temperature without external heating or vacuum treatment. During solvent evaporation, the nanoparticles were deposited onto the substrate surfaces, forming uniform nanoparticle layers suitable for structural, morphological, compositional, and vibrational characterization.

The XRD and Raman results suggest that the PLAL process largely preserves the crystalline GaSe phase while transforming the bulk crystal into nanoscale structures.

2.2 Characterization techniques

The structural properties of the synthesized GaSe nanoparticles were investigated by X-ray diffraction (XRD) using a Rigaku MiniFlex 600 diffractometer equipped with Ni-filtered Cu Kα radiation (λ = 0.15406 nm). The surface morphology, microstructural features, and elemental composition of the GaSe nanoparticle-derived films were examined using a Vega Tescan scanning electron microscope (SEM) coupled with an energy-dispersive X-ray spectroscopy (EDS) system. SEM analysis provided information on surface topology, particle distribution, and film uniformity, while EDS measurements were employed to verify the elemental composition and chemical purity of the samples.

Raman spectroscopic analysis was performed using an EnSpectr R532 Raman spectrometer (Enhanced Spectrometry Inc., USA) with a 532-nm laser-excitation source to probe the phonon modes, assess crystallinity, and verify the structural integrity of the GaSe nanoparticles in comparison with bulk GaSe crystals.

3 RESULTS

3.1 XRD Analysis of GaSe Nanoparticles on Glass and Silicon Substrates

The crystal structure and phase composition of the GaSe nanoparticles synthesized by pulsed-laser ablation

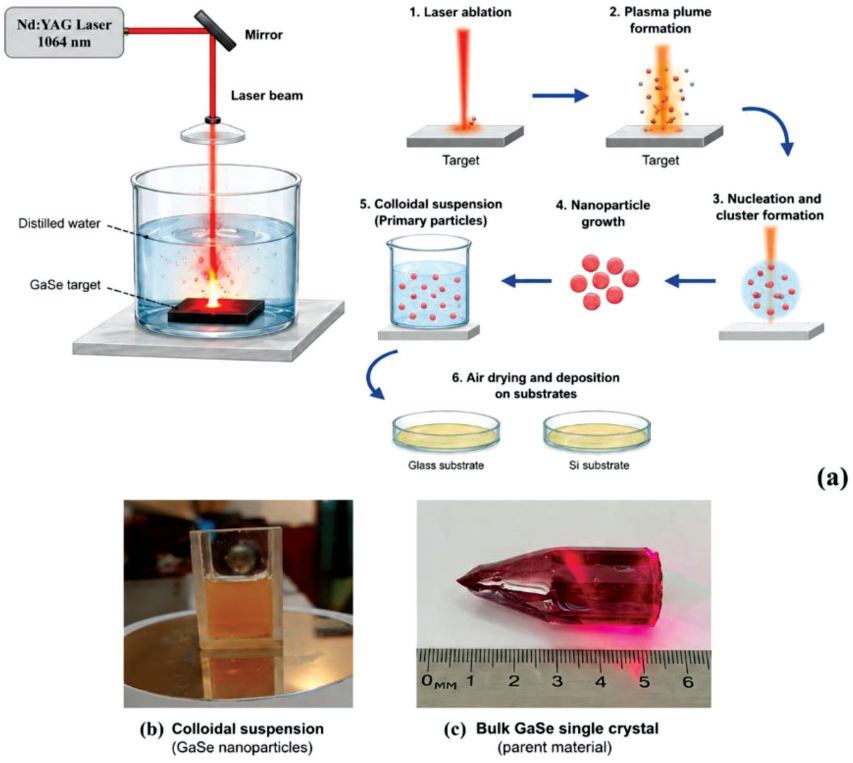

Figure 1: a) Schematic representation of the PLAL setup and proposed nanoparticle formation mechanism, including laser ablation, plasma-plume formation, nucleation, nanoparticle growth, colloidal suspension formation, and deposition on glass and Si substrates. b) Photograph of the GaSe colloidal suspension after ablation in distilled water. c) Bulk GaSe single crystal used as the parent target material.

in liquid (LAL) were investigated by X-ray diffraction (XRD) after deposition on two different substrates: glass and single-crystal silicon. The diffraction patterns corresponding to GaSe/glass and GaSe/Si samples are presented in **Figure 2a** and **Figure 2b**, respectively. A comparison of these patterns clearly reveals the influence of the substrate on the observed diffraction features, while confirming the formation of crystalline GaSe nanoparticles in both cases.

For the GaSe nanoparticles deposited on the glass substrate (**Figure 2a**), several diffraction peaks are observed at approximately $2\theta \approx 9.77°$, 22.74°, 28.88°, 30.83°, 49.09°, 52.85°, 58.81°, and 63.34°. These reflections can be indexed to the hexagonal ε-GaSe phase and are in good agreement with the standard diffraction data reported in the PDF database (JCPDS card No. 37-931). The dominant peak at $2\theta \approx 22.74°$ corresponds to the (004) crystallographic plane of hexagonal GaSe.[19] The strong intensity of this reflection indicates a pronounced preferential orientation along the c-axis, which is characteristic of layered GaSe crystals. The presence of several (00l) reflections further confirms that the fundamental layered structure composed of Se–Ga–Ga–Se tetralayers stacked via weak van der Waals interactions is preserved even after laser-induced ablation and subsequent plasma-mediated condensation into nanoscale domains.[20]

In contrast, the XRD pattern of the GaSe nanoparticles deposited on the silicon substrate (**Figure 2b**) is dominated by a very intense diffraction peak located at approximately $2\theta \approx 69.6°$, which corresponds to the (400) reflection of the single-crystal Si substrate.[21] The sharp and high-intensity nature of this peak reflects the excellent crystallinity and strong diffraction contribution of the silicon substrate. In addition to this substrate-related peak, several weaker reflections are detected at approximately $2\theta \approx 22.6°$, 33.3°, and 62.0°, which can be attributed to the crystalline phase of hexagonal GaSe. These peaks confirm the successful deposition of GaSe nanoparticles on the Si surface and the formation of a GaSe nanoparticle/Si heterostructure.

The difference in diffraction intensities between the two samples is mainly attributed to the nature of the substrates. For the GaSe/glass sample, the amorphous glass substrate contributes only a weak background signal, allowing the GaSe diffraction peaks to be clearly observed. In contrast, the highly crystalline silicon substrate produces a strong diffraction peak at $2\theta \approx 69.6°$, which partially masks the weaker reflections from the nanoparticle layer. Consequently, the GaSe peaks appear less pronounced in the GaSe/Si sample. Such behavior is commonly observed for nanostructured films deposited on highly crystalline substrates.[22]

Additionally, the GaSe diffraction peaks in both samples exhibit noticeable broadening compared to those of bulk GaSe crystals. Such peak broadening is characteristic of nanoscale materials and is generally attributed to the small crystallite size and possible lattice strain effects. The average crystallite size of the GaSe nanoparticles was estimated using the Debye–Scherrer equation:

$$D = \frac{K\lambda}{\beta \cos\theta} \tag{1}$$

where D is the crystallite size, K is the shape factor (0.9), λ is the X-ray wavelength (0.15406 nm for Cu Kα radiation), β is the full width at half maximum (FWHM) of the selected diffraction peak corrected for instrumental broadening, and θ is the Bragg diffraction angle. The crystallite size was estimated from several well-resolved diffraction peaks of the hexagonal ε-GaSe phase. For each selected reflection, the full width at half maximum (FWHM) was determined after baseline correction, and the Debye–Scherrer equation was applied individually. The reported crystallite size range represents the values obtained from these selected reflections. The calculated crystallite sizes fall within the range of approximately 10–30 nm, confirming the successful formation of GaSe nanoparticles during the laser ablation process.

Importantly, no additional diffraction peaks associated with metallic gallium, selenium, or gallium oxide

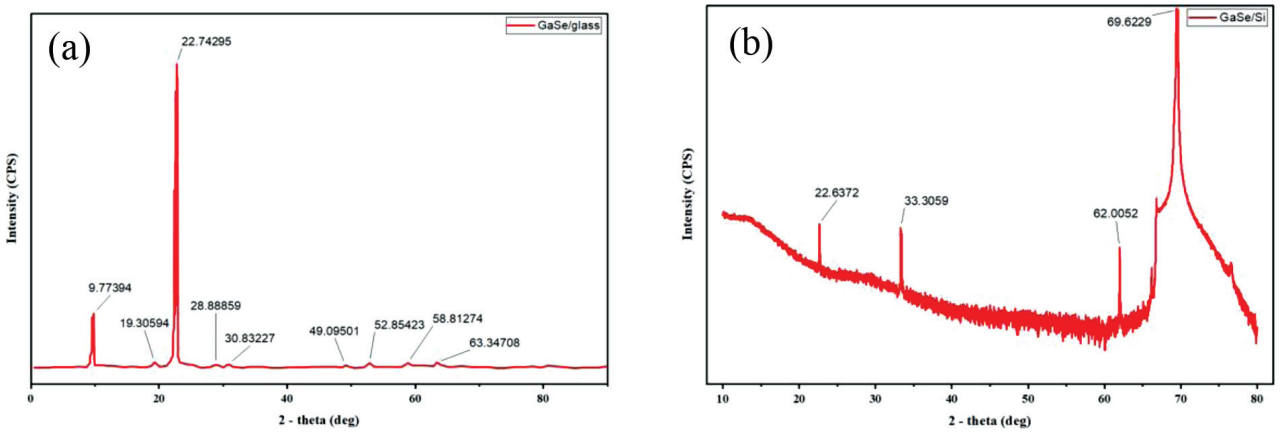

Figure2: XRD patterns of GaSe nanoparticles deposited on: a) glass and b) silicon substrates

phases were detected in either diffraction pattern, indicating that the synthesized nanoparticles possess good phase purity within the detection limits of the XRD technique.[23,24]

Overall, the comparative XRD analysis demonstrates that pulsed-laser ablation in liquid enables the formation of crystalline GaSe nanoparticles that retain the intrinsic hexagonal layered structure of the parent material. While the amorphous glass substrate allows clear observation of GaSe diffraction peaks, the highly crystalline silicon substrate introduces strong substrate-related reflections that dominate the diffraction pattern. Nevertheless, the presence of characteristic GaSe reflections in both samples confirms the successful deposition of GaSe nanoparticles and highlights the formation of GaSe nanoparticle/substrate heterostructures.

3.2 Surface morphology and elemental composition of GaSe nanoparticles

3.2.1 Surface morphology and elemental composition of GaSe nanoparticles on glass substrate

The surface morphology of the GaSe nanoparticles deposited on the glass substrate was investigated by scanning electron microscopy (SEM), as shown in **Figure 3a**. The SEM micrograph reveals a relatively dense and homogeneous distribution of particles across the substrate surface. Most particles exhibit a quasi-spherical morphology with distinguishable boundaries, indicating the formation of nanoscale GaSe structures during the pulsed-laser ablation in liquid process. Localized particle agglomeration is also observed, which is commonly reported for ligand-free nanoparticles synthesized by physical methods due to their high surface energy and tendency toward interparticle interaction. No large debris or irregular micron-sized fragments are observed within the examined area, suggesting that the deposited layer is predominantly composed of fine particles.

To evaluate the particle size distribution, approximately 60 representative particles were selected from the SEM image and measured using image-analysis software. The corresponding histogram (**Figure 3b**) shows that the particle sizes are mainly distributed in the range of approximately 60–180 nm, with an average particle diameter of about 118 nm. These results confirm the formation of particles within the nanoscale regime. The observed particle dimensions and surface morphology are consistent with the nanoscale characteristics expected for laser-generated GaSe nanostructures and may contribute to modifications in their structural and vibrational properties. The larger particle sizes observed by SEM compared with the crystallite sizes estimated from XRD suggest that the deposited particles consist of aggregates of smaller nanocrystalline domains. Such differences are commonly observed in nanomaterials synthesized by PLAL and other methods because the Debye–Scherrer equation estimates the size of coherent diffraction domains (crystallites), whereas SEM measures the overall particle dimensions, which may comprise several crystallites aggregated during nanoparticle growth, deposition, and drying. Similar observations have been widely reported for laser-generated semiconductor nanoparticles and other nanocrystalline systems.[25]

The elemental composition of the GaSe nanoparticles deposited on the glass substrate was analyzed by energy-dispersive X-ray spectroscopy (EDS), and the corresponding spectrum is displayed in **Figure 4**. Prominent characteristic peaks associated with Ga and Se are clearly observed, confirming the preservation of the GaSe chemical composition following laser ablation in liquid.[26] In addition, a noticeable oxygen signal is detected. This oxygen contribution is primarily attributed to the SiO_2-based glass substrate. However, partial surface oxidation of the GaSe nanoparticles during the PLAL process or subsequent exposure to the ambient atmosphere after deposition cannot be completely excluded. Such surface oxidation has been reported for

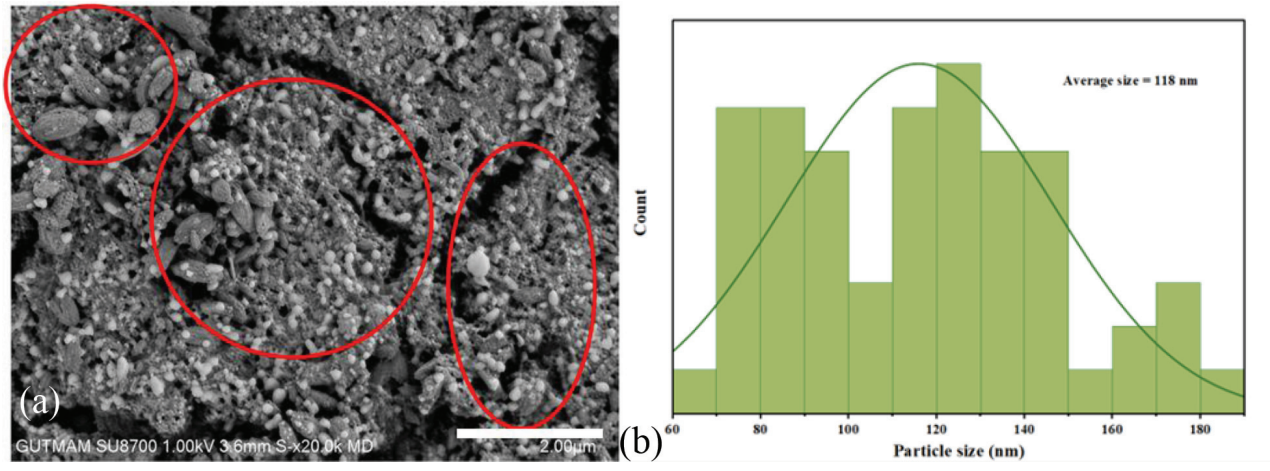

Figure3: a) SEM micrograph of GaSe nanoparticles deposited on the glass substrate. The red circles mark the regions of interest (ROIs) used for particle size measurements in the statistical size distribution analysis. b) Particle size distribution of the GaSe nanoparticles on the glass substrate.

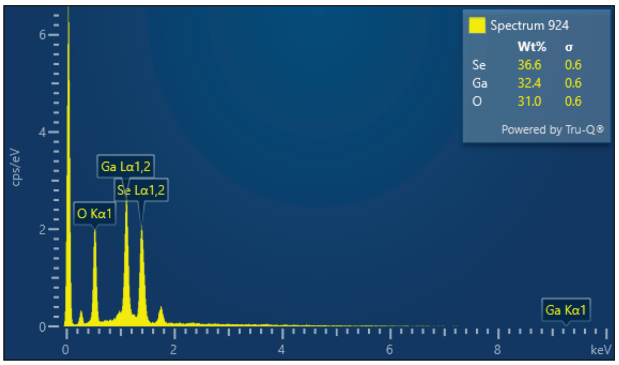

Figure 4: EDS results of GaSe nanoparticles on glass substrate

semiconductor nanoparticles synthesized by PLAL because of their high surface-to-volume ratio and the reactive environment generated during laser ablation in aqueous media.[17,18] Quantitative EDS analysis yields approximately 36.6 *w*/% Se, 32.4 *w*/% Ga, and 31.0 *w*/% O. The dominance of the Ga and Se peaks verifies the successful formation of GaSe nanostructures. Therefore, the detected oxygen is attributed mainly to the SiO_2-based glass substrate and, to a lesser extent, to possible surface oxidation of the nanoparticles. Furthermore, the absence of oxide-related diffraction peaks in the XRD patterns suggests that any oxidation is limited to a thin surface layer and does not significantly alter the crystalline ε-GaSe phase. The absence of impurity-related elemental peaks further confirms the high purity of the nanomaterials produced via laser ablation.

3.2.2 Surface morphology and elemental composition of GaSe nanoparticles on silicon substrate

The surface morphology of the GaSe nanoparticles deposited on the silicon (Si) substrate was examined by SEM, as shown in **Figure 5a**. The SEM image reveals a relatively uniform distribution of particles across the Si surface, with most particles exhibiting a quasi-spherical morphology and distinguishable boundaries. Similar to the glass-supported sample, partial particle agglomeration is observed, which is commonly encountered in ligand-free nanoparticles synthesized by physical methods due to their high surface energy and tendency toward interparticle interactions. The deposited layer appears to consist predominantly of fine particles distributed over the substrate surface, with no obvious large debris or micron-sized fragments observed within the examined region.

To evaluate the particle size distribution, approximately 60 representative particles were selected from the SEM micrograph and measured using image-analysis software. The resulting histogram (**Figure 5b**) indicates that the particle sizes are mainly distributed within the range of approximately 60–188 nm, with an average particle diameter of about 111 nm. These results confirm the formation of particles within the nanoscale regime. Compared with the glass-supported sample (average particle size ≈118 nm), the slightly smaller average size observed on the Si substrate may reflect differences in the nanoparticle distribution and aggregation during the deposition and drying processes. Overall, the SEM observations confirm the successful deposition of GaSe nanoparticles on the silicon substrate and demonstrate a morphology comparable to that observed on the glass. The larger particle dimensions observed by SEM relative to the crystallite sizes estimated from XRD indicate that individual particles may be composed of multiple nanocrystalline domains aggregated during deposition and drying.

The elemental composition of the GaSe nanoparticles deposited on the Si substrate was examined by energy-dispersive X-ray spectroscopy (EDS), and the corresponding spectrum is displayed in **Figure 6**. Characteristic peaks corresponding to Ga and Se are clearly visible, confirming the presence of GaSe nanostructures.

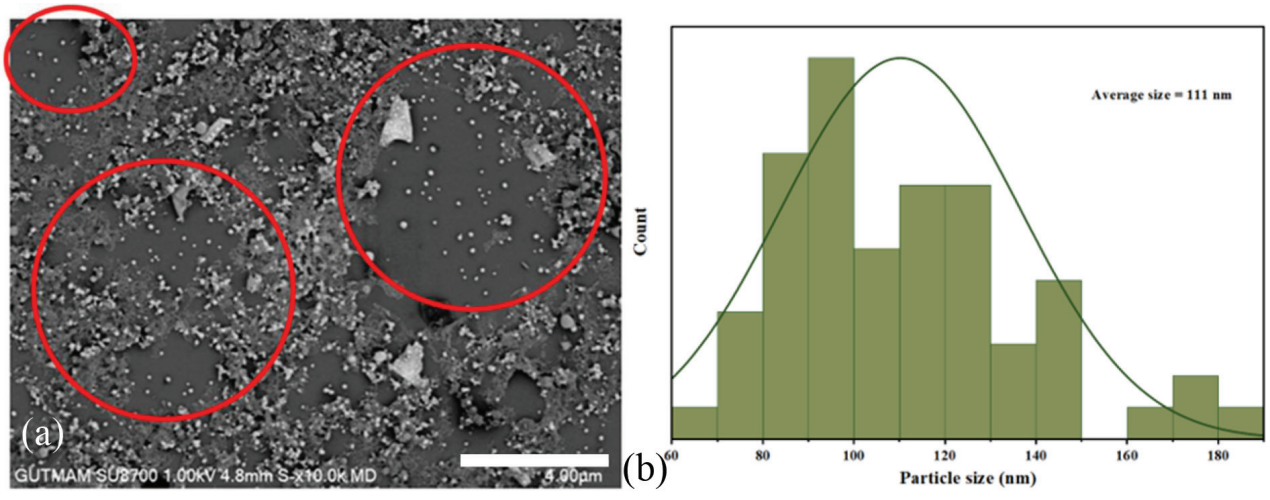

Figure 5: a) SEM micrograph of GaSe nanoparticles deposited on the silicon substrate. The red circles mark the regions of interest (ROIs) used for particle size measurements in the statistical size distribution analysis. b) Particle size distribution of the GaSe nanoparticles on the silicon substrate.

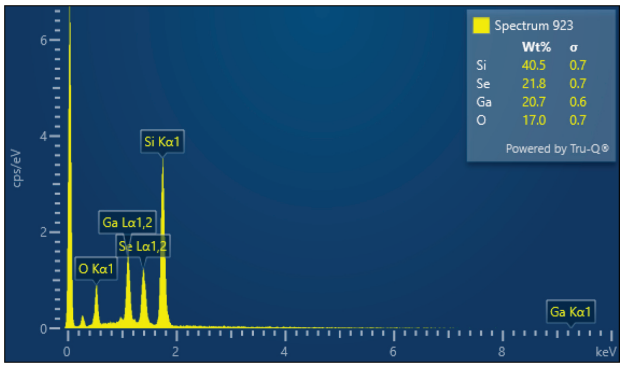

Figure 6: EDS results of GaSe nanoparticles on silicon substrate

In addition, a strong Si peak is observed, originating from the underlying silicon substrate, together with a moderate oxygen signal. The detected oxygen is mainly attributed to the native SiO_2 layer naturally present on the silicon surface. Nevertheless, partial surface oxidation of the GaSe nanoparticles during the PLAL process or subsequent exposure to ambient atmosphere after deposition cannot be completely excluded. Such surface oxidation has been reported for semiconductor nanoparticles synthesized by PLAL because of their high surface-to-volume ratio and the reactive environment generated during laser ablation in aqueous media. Quantitative EDS analysis indicates approximately 40.5 *w*/% Si, 21.8 *w*/% Se, 20.7 *w*/% Ga, and 17.0 *w*/% O. The prominent Si contribution is associated with the substrate, while the combined Ga and Se contents verify the successful deposition of GaSe nanoparticles. Therefore, the detected oxygen is mainly associated with the native SiO_2 layer on the silicon substrate, although a minor contribution from surface oxidation of the nanoparticles may also be present. Furthermore, the absence of oxide-related diffraction peaks in the XRD patterns suggests that any oxidation is confined to a thin surface layer and does not significantly affect the crystalline ε-GaSe phase. No impurity-related elemental peaks were detected, further demonstrating the chemical purity of the laser-ablated GaSe nanomaterials.

3.3 Raman analysis of GaSe nano particles

3.3.1 Raman analysis of GaSe nanoparticles on glass substrate

Raman spectroscopy was employed to investigate the structural integrity and vibrational properties of GaSe nanoparticles deposited on the glass substrate after pulsed-laser ablation in liquid (**Figure 7**). The Raman spectrum exhibits distinct vibrational bands at approximately (135.6, 212.7, 237.4, 254.2, 308.2, 441.4 and 464.0) cm^{-1}, indicating that the characteristic lattice framework of GaSe is largely preserved after nanoparticle formation.

The most prominent Raman features are observed at ≈135.6 cm^{-1} and ≈308.2 cm^{-1}, which are commonly assigned to the $A_1(1)/A_1g(1)$ and $A_1(2)/A_1g(2)$ out-of-plane optical phonon modes of layered GaSe, respectively.[27–29] The clear presence of these characteristic modes confirms that the deposited nanomaterial retains the crystalline GaSe phase following laser ablation and deposition. In addition, the band observed at ≈212.7 cm^{-1} is attributed to an E-type in-plane vibrational mode of GaSe.[30] Since this mode is sensitive to interlayer interactions and stacking arrangement, its presence suggests that the layered nature of GaSe is maintained in the nanoparticle state.

Compared with bulk GaSe crystals, the nanoparticle sample exhibits additional Raman features in the 230–260 cm^{-1} region, particularly at ≈237.4 cm^{-1} and ≈254.2 cm^{-1}. In bulk GaSe, Raman spectra are typically dominated by a limited number of strong first-order phonon modes, whereas additional weak features may become more apparent in nanostructured materials. The appearance of these bands may be associated with nanoscale effects such as phonon confinement, local strain, surface reconstruction, structural disorder, or possible stacking variations introduced during the laser ablation and rapid cooling processes. Similar disorder-activated Raman features have been reported in nanostructured layered semiconductors, where reduced crystallite dimensions and increased surface contributions can relax Raman selection rules and enhance otherwise weak vibrational modes.[27–30]

Additional bands observed at ≈441.4 cm^{-1} and ≈464.0 cm^{-1} are not among the principal first-order Raman modes of bulk GaSe. These features may therefore be attributed to second-order Raman scattering processes (overtones and/or combination modes) or to surface-related vibrational contributions that become more pronounced in nanostructured materials. Such higher-order and disorder-assisted scattering processes are frequently observed in semiconductor nanoparticles due to their increased surface-to-volume ratio and the modified phonon dynamics.

The Raman interpretation is also consistent with the EDS analysis of the GaSe/glass sample, which revealed

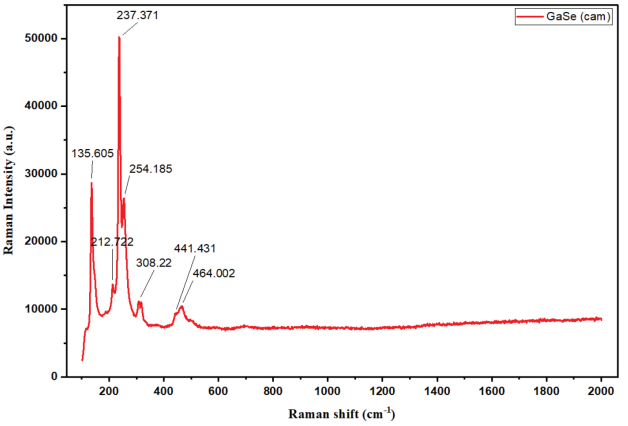

Figure 7: Raman spectrum GaSe nanoparticles deposited on a glass substrate

elemental contents of approximately 36.6 *w*/% Se, 32.4 *w*/% Ga, and 31.0 *w*/% O. The oxygen signal is primarily attributed to the SiO_2-based glass substrate and, to a lesser extent, possible surface oxidation or adsorption occurring during ambient drying. Such surface-related effects may contribute to modifications in the Raman background and the appearance of additional weak vibrational features.

Overall, the Raman spectrum confirms the preservation of the characteristic GaSe phonon modes after PLAL synthesis while revealing additional nanoscale-related vibrational features. The emergence of bands in the 237–254 cm^{-1} region and the appearance of higher-frequency features at 441–464 cm^{-1} suggest that nanoparticle formation introduces structural and surface-related modifications compared with bulk GaSe, while maintaining the fundamental layered crystal framework.

3.3.2 Raman analysis of GaSe nanoparticles on silicon substrate

The vibrational properties of the GaSe nanoparticles synthesized by pulsed laser ablation in liquid and subsequently deposited on a silicon substrate were investigated by Raman spectroscopy (**Figure 8**). The Raman spectrum exhibits distinct bands at approximately (135.6, 212.7, 236.1, 308.2, 315.9, 441.4, 464.0 and 522.6) cm^{-1}. The presence of the characteristic GaSe phonon modes indicates that the crystalline GaSe phase is preserved after laser ablation and deposition, while additional Raman features suggest the influence of nanoscale and substrate-related effects.

The dominant Raman bands observed at ≈135.6 cm^{-1} and ≈308.2 cm^{-1} are characteristic of layered GaSe and are commonly assigned to the $A_1(1)/A_1g(1)$ and $A_1(2)/A_1g(2)$ out-of-plane optical phonon modes, respectively.[27–29] Their clear observation confirms that the layered crystal framework of GaSe is retained in the nanoparticle form. In addition, the band at ≈212.7 cm^{-1} corresponds to an E-type in-plane vibrational mode of GaSe, which is known to be sensitive to interlayer interactions and stacking arrangement.[30] The persistence of this mode further supports the preservation of the layered structure following nanoparticle formation.

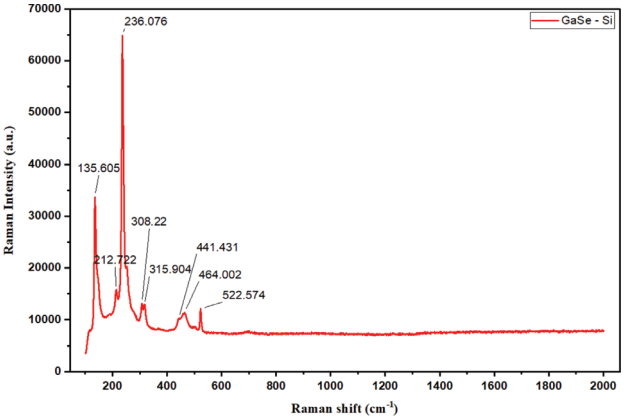

Figure 8: Raman spectrum GaSe nanoparticles deposited on a silicon substrate

A prominent Raman peak is observed at ≈522.6 cm^{-1}, which is attributed to the first-order Raman mode of the silicon substrate.[31] The appearance of this feature is expected and indicates that the Raman signal contains contributions from both the deposited nanoparticle layer and the underlying substrate, particularly in regions where the nanoparticle coverage may be relatively thin.

Comparison with the Raman spectrum of GaSe nanoparticles deposited on the glass substrate reveals a substrate-dependent vibrational response. While the principal GaSe modes (≈135.6, ≈212.7, and ≈308.2 cm^{-1}) are present on both substrates, differences are observed in the intermediate spectral region. In particular, the glass-supported sample exhibits an additional band near ≈254.2 cm^{-1}, whereas the Si-supported sample shows a distinct feature at ≈315.9 cm^{-1}. These differences may be associated with variations in local structural disorder, phonon confinement effects, interfacial strain, nanoparticle packing, or substrate-induced modifications of the Raman scattering process. However, the precise origin of these features requires further investigation.

The Raman interpretation is consistent with the EDS analysis of the GaSe/Si sample, which revealed elemental contents of approximately 40.5 *w*/% Si, 21.8 *w*/% Se, 20.7 *w*/% Ga, and 17.0 *w*/% O. The strong silicon contribution originates from the substrate, while the oxygen signal may be associated with the native SiO_2 layer and minor surface oxidation or adsorption processes occurring during drying under ambient conditions.

In addition to peak positions, noticeable differences in relative Raman intensities are observed between the samples deposited on Si and glass substrates. The mode near ≈236 cm^{-1} exhibits enhanced intensity in the Si-supported sample, whereas the glass-supported sample shows a broader distribution of Raman intensity in the 237–254 cm^{-1} region. Such variations may reflect differences in nanoparticle arrangement, local strain fields, surface morphology, or optical interactions at the nanoparticle–substrate interface. These observations indicate that the substrate can influence the vibrational response of deposited GaSe nanoparticle layers.

Overall, the Raman results confirm that the characteristic GaSe phonon modes are retained after PLAL synthesis and deposition on silicon. At the same time, substrate-dependent spectral variations demonstrate that the vibrational properties of GaSe nanoparticle layers are influenced by the supporting substrate, highlighting the importance of substrate–nanoparticle interactions in determining the Raman response of these nanostructures.

To facilitate a comparison between bulk GaSe and the synthesized nanoparticles deposited on different substrates, the observed Raman modes are summarized in **Table 1**. As shown in the table , the characteristic Raman fingerprints of GaSe, namely the $A_1(1)$ (≈135.6 cm^{-1}), *E* (≈212.7 cm^{-1}), and $A_1(2)$ (≈308.2 cm^{-1}) modes, are

Table 1: Comparison of Raman modes observed in bulk GaSe and GaSe nanoparticles deposited on different substrates

Raman mode	Bulk GaSe (literature) (cm^{-1})	GaSe/glass (cm^{-1})	GaSe/Si (cm^{-1})	Assignment
$A_1(1)$	134–136	135.6	135.6	Out-of-plane optical phonon
E mode	212–214	212.7	212.7	In-plane vibration
Additional mode	–	237.4	236.1	Disorder-activated / nanoscale-related
Additional mode	–	254.2	–	Disorder-related feature
$A_1(2)$	308–310	308.2	308.2	Out-of-plane optical phonon
Additional mode	–	–	315.9	Possible substrate/interface effect
Higher-order band	–	441.4	441.4	Second-order scattering
Higher-order band	–	464.0	464.0	Second-order scattering
Si substrate peak	–	–	522.6	First-order Si phonon

preserved after laser ablation in liquid and subsequent deposition on both substrates. Additional Raman features observed in the nanoparticle samples indicate nanoscale-induced modifications and possible substrate-related effects.

4 CONCLUSIONS

GaSe nanoparticles were successfully synthesized by pulsed-laser ablation in liquid (PLAL) using bulk GaSe single crystals as target materials. XRD analysis confirmed the preservation of the hexagonal ε-GaSe phase after laser processing, while peak broadening indicated the formation of nanocrystalline domains. SEM observations revealed quasi-spherical nanoparticles with characteristic dimensions in the nanometer range, and EDS measurements verified the presence of Ga and Se as the main constituent elements without any evidence of impurity phases. Raman spectroscopy demonstrated that the characteristic GaSe phonon modes were retained after nanoparticle formation, indicating preservation of the layered crystal structure. At the same time, additional Raman features and intensity variations were observed depending on the supporting substrate, suggesting that substrate–nanoparticle interactions influence the vibrational response of the deposited layers. In particular, glass-supported and Si-supported samples exhibited distinct Raman signatures that may be associated with differences in local disorder, interfacial strain, and surface-related effects.

Overall, the results demonstrate that PLAL provides an effective route for producing crystalline GaSe nanoparticles, while maintaining the fundamental structural characteristics of the parent material. The observed substrate-dependent vibrational behavior highlights the importance of substrate selection for the characterization and potential implementation of GaSe nanostructures in future optoelectronic and nanophotonic applications.

Acknowledgments

The authors acknowledge the financial support from the Slovenian Research Agency (research core funding No. P2-0132).

Data-availability statement

The data supporting the findings of this study are available within the article. The raw datasets generated and analyzed during the current study, are available in the Zenodo repository:
https://zenodo.org/records/22078513.[32]

Generative AI statement

During the preparation of this manuscript, the authors used AI to improve the language, grammar, and readability of the text. The authors reviewed and edited the output as necessary and take full responsibility for the content of the publication.

6 REFERENCES

[1] H. Wang, H. Wu, W. Lin, B. Zhang, X. Li, Y. Zhang, S. Fan, C. Dang, Y. Zhu, S. Zhao, X. Zhou, Orientation-dependent large plasticity of single-crystalline gallium selenide, Cell Rep. Phys. Sci., 3 (**2022**) 4, 100875. doi:10.1016/j.xcrp.2022.100816

[2] T. H. Fang, D. Q. Doan, Effects of surface defects on mechanical properties and fracture mechanism of gallium selenide/graphene heterostructure, Mech. Mater., 180 (**2023**), 104610. doi:10.1016/j.mechmat.2023.104610

[3] H. Arora, A. Erbe, Recent progress in contact, mobility, and encapsulation engineering of InSe and GaSe, InfoMat, 3 (**2021**) 6, 662–693. doi:10.1002/inf2.12160

[4] W. Jie, J. Hao, Two-dimensional layered gallium selenide: preparation, properties, and applications, Adv. 2D Mater., (**2016**), 1–36. doi:10.1002/9781119242635

[5] J. Grzonka, M. S. Claro, A. Molina-Sánchez, S. Sadewasser, P. J. Ferreira, Novel polymorph of GaSe, Adv. Funct. Mater., 31 (**2021**) 48, 2104965. doi:10.1002/adfm.202104965

[6] S. Mou, A. Rubano, D. Paparo, Terahertz hyper-Raman time-domain spectroscopy of gallium selenide and its application in terahertz detection, Appl. Phys. Lett., 115 (**2019**) 21. doi:10.1063/1.5115986

[7] M. Song, N. An, Y. Zou, Y. Zhang, W. Huang, H. Hou, X. Chen, Epitaxial growth of 2D gallium selenide flakes for strong nonlinear optical response and visible-light photodetection, Front. Phys., 18 (**2023**) 5, 52302. doi:10.1007/s11467-023-1277-3

[8] M. Nakamura, H. Nakamura, K. Shimamura, N. Ohashi, Growth and characterization of a gallium monosulfide (GaS) single crystal using the Bridgman method, J. Cryst. Growth, 573 (**2021**), 126303. doi:10.1016/j.jcrysgro.2021.126303

[9] J. Ko, et al., Electronic effects of nano-confinement in functional organic and inorganic materials for optoelectronics, Chem. Soc. Rev., 50 (**2021**) 5, 3585–3628. doi:10.1039/D0CS01501F

[10] A. F. Palmstrom, P. K. Santra, S. F. Bent, Atomic layer deposition in nanostructured photovoltaics: tuning optical, electronic and surface properties, Nanoscale, 7 (**2015**) 29, 12266–12283. doi:10.1039/C5NR02080H

[11] H. Tu, V. Chikan, D. F. Kelley, Electron and hole intraband spectroscopy of GaSe nanoparticles, J. Phys. Chem. B, 107 (2003) 38, 10389–10397. doi:10.1021/jp034297

[12] A. G. Kyazym-Zade, et al., Structure, optical, and luminescent properties of GaSe nanoparticles, Nanotechnol. Russ., 10 (**2015**) 9, 794–801. doi:10.1134/S1995078015050122

[13] S. Ramanathan, et al., Nanoparticle synthetic methods: strength and limitations, in: Nanoparticles in Analytical and Medical Devices, Elsevier, 2021, 31–43. doi:10.1016/B978-0-12-821163-2.00002-9

[14] K. Hachem, et al., Methods of chemical synthesis in the synthesis of nanomaterial and nanoparticles by the chemical deposition method: a review, BioNanoScience, 12 (**2022**) 3, 1032–1057. doi:10.1007/s12668-022-00996-w

[15] I. Y. Khairani, et al., Green nanoparticle synthesis at scale: a perspective on overcoming the limits of pulsed laser ablation in liquids for high-throughput production, Phys. Chem. Chem. Phys., 25 (**2023**) 29, 19380–19408. doi:10.1039/D3CP01214J

[16] Y. Monsa, et al., A simple strategy for enhanced production of nanoparticles by laser ablation in liquids, Nanotechnology, 31 (**2020**) 23, 235601. doi:10.1088/1361-6528/ab78ac

[17] E. Fazio, et al., Nanoparticles engineering by pulsed laser ablation in liquids: concepts and applications, Nanomaterials, 10 (**2020**) 11, 2317. doi:10.3390/nano10112317

[18] A. H. Attallah, et al., Effect of liquid and laser parameters on fabrication of nanoparticles via pulsed laser ablation in liquid with their applications: a review, Plasmonics, 18 (**2023**) 4, 1307–1323. doi:10.1007/s11468-023-01852-7

[19] N. Q. Diep, Y. X. Chen, D. L. Nguyen, M. N. Duong, S. K. Wu, C. W. Liu, H. C. Wen, W. C. Chou, J. Y. Juang, Y. J. Hsu, V. Q. Le, Monotonous alloying-driven band edge emission in two-dimensional hexagonal GaSe1-xTex semiconductors for visible to near-infrared photodetection, J. Mater. Chem. C, 11 (**2023**) 5, 1772–1781. doi:10.1039/D2TC04252E

[20] S. Y. Sarkisov, A. V. Kosobutsky, S. D. Shandakov, Effect of van der Waals interactions on the structural and binding properties of GaSe, J. Solid State Chem., 232 (**2015**), 67–72. doi:10.1016/j.jssc.2015.09.002

[21] L. Wang, X. Gu, Y. Zhao, M. Wei, C. Huang, Y. Qiang, Enhanced photoelectrochemical performance of Si nanowires by etching a single-crystal Si (100) wafer, Appl. Surf. Sci., 448 (**2018**), 126–132. 10.1016/j.apsusc.2018.04.108

[22] V. M. Salmanov, et al., Determination of nonlinear absorption in InSe nanoparticles synthesized by laser ablation in liquid. doi:10.30546/209501.2024.01.4.067

[23] P. Patil, J. Park, S. Y. Lee, J. K. Park, S. H. Cho, White light generation from single gallium oxide nanoparticles co-doped with rare-earth metals, Appl. Sci. Converg. Technol., 23 (**2014**) 5, 296–300. doi:10.5757/ASCT.2014.23.5.296

[24] M. A. Fresneda, J. D. Martín, J. G. Bolívar, M. V. Cantos, G. Bosch-Estévez, M. F. Moreno, M. L. Merroun, Green synthesis and biotransformation of amorphous Se nanospheres to trigonal 1D Se nanostructures: impact on Se mobility within the concept of radioactive waste disposal, Environ. Sci. Nano, 5 (**2018**) 9, 2103–2116. doi:10.1039/C8EN00221E

[25] P. Bindu, S. Thomas, Estimation of lattice strain in ZnO nanoparticles: X-ray peak profile analysis, J. Theor. Appl. Phys., 8 (**2014**) 4, 123–134. doi:10.1007/s40094-014-0141-9

[26] V. M. Salmanov, et al., Preparation of Gallium Selenide Nanoparticles by Laser Ablation in Liquid, Russ. J. Phys. Chem. A, 98 (**2024**) 3, 479–483. doi:10.1134/S0036024424030257

[27] W. Chu, et al., Single crystal growth of GaSe via bismuth flux method and its air-stability, J. Cryst. Growth, 562 (**2021**), 126088. doi:10.1016/j.jcrysgro.2021.126088

[28] M. Al-Hattab, et al., Structural properties and vibrational modes of different polytypes of gallium selenide crystals (ε, β, γ, δ): insights from a DFT study, Indian J. Phys., 98 (2024) 14, 4933–4947. doi:10.1007/s12648-024-03248-7

[29] M. K. Niranjan, Significance of Coulomb interaction in interlayer coupling, polarized Raman intensities, and infrared activities in the layered van der Waals semiconductor GaSe, Phys. Rev. B, 103 (**2021**) 19, 195437. doi:10.1103/PhysRevB.103.195437

[30] M. Bejani, et al., Lattice vibrations and electronic properties of GaSe nanosheets from first principles, Phys. Rev. Mater., 3 (**2019**) 12, 124003. doi:10.1103/PhysRevMaterials.3.124003

[31] V. V. Kidalov, et al., Properties of SiC films obtained by the method of substitution of atoms on porous silicon, ECS J. Solid State Sci. Technol., 7 (**2018**) 4, P158. DOI 10.1149/2.0061804jss

[32] M. Conradi, V. Salmanov, R. Mamedov, A. Guseinov, F. Ahmedova, L. Balayeva, M. B. Baghirov, A. Khaligzade, Z. Addayeva, (2026). Structural and Vibrational Properties of PLAL-Synthesized GaSe Nanoparticles on Different Substrates [Dataset]. Zenodo. https://doi.org/10.5281/zenodo.22078513